World Journal of Engineering Research and Technology
WJERT
www.wjert.org
SJIF Impact Factor: 4.326

NUMERICAL INVESTIGATION OF BLOOD FLOW THROUGH STENOTIC ARTERY

Mohammed Nasir Uddin*[1] and M. A. Alim[2]

[1]Department of Information and Communication Technology (ICT), Bangladesh University of Professionals (BUP), Bangladesh.

[2]Department of Mathematics, Bangladesh University of Engineering & Technology (BUET), Bangladesh.

Article Received on 20/08/2017 **Article Revised on 10/09/2017** **Article Accepted on 01/10/2017**

***Corresponding Author**
Mohammed Nasir Uddin
Department of Information and Communication Technology (ICT), Bangladesh University of Professionals (BUP), Bangladesh.

ABSTRACT

The aim of this paper is to investigate the significance of stenosis effects on blood flow and measures the non-Newtonian characteristics of blood flow in blood vessels. At present work, the models are studied for the Newtonian and Non-Newtonian models as well as their generalized modifications. The governing system of equations is based on incompressible Navier-Stokes equations which are generalized to consider viscoelasticity and shear-thinning properties of blood flow. The numerical solution of the system of governing equations is obtained by Finite element method. Mathematical tests are performed on an idealized stenosis and a realistic stenosed carotid bifurcation reconstructed from medical images. Model sensitivity tests are achieved with respect to the characteristic flow rate to evaluate its impact on the observed non-Newtonian effects. The numerical simulation is performed for various dimensionless numbers (Reynold numbers, Re=1-1050 and Weissenberg numbers, Wi= 0-1.0) at flow rates 0.5 cm^3/s with good convergence of the iterative scheme. The blood flow simulations indicate that non-Newtonian behavior has considerable effects on instantaneous flow patterns. The blood flow patterns are shown in terms of velocity and pressure contour line. Various effects for these models are presented graphically.

KEYWORDS: Non-Newtonian fluid, Viscoelasticity, Stenosis Artery, Oldroyd-B model, Finite element method.

INTRODUCTION

Nowadays the fatal cardiovascular disease arteriosclerosis or stenosis and aneurysm affects the flow of blood in the arteries and leads to serious circulatory disorders, this area of biomechanics has been receiving the attention of researchers during the recent decades[8,15]. At present time medical researchers, bioengineers and numerical scientists join efforts with the purpose of providing numerical simulations of human blood flow system in different conditions. In our blood circulation system, there are some strong hemodynamical features that can change in the rheological properties of blood and its components. It plays a major role in the development and progression of atherosclerotic plaques and other arterial lesions[19]. In any physiological and pathological situations, the numerical study is an important tool for the interpretation and analysis of the circulatory system and can capture the rheological response of blood over a range of physiological flow conditions accurately[9]. Stenosis developed in the arteries pertaining to brain can cause cerebral strokes and the one developed in the coronary arteries can cause myocardial infarction which leads to heart failure[11]. It has been reported that the fluid dynamical properties of blood flow through nonuniform cross section of the arteries play a major role in the fundamental understanding and treatment of many cardiovascular diseases[21]. The analysis of blood flow through tapered tubes is very important in understanding the behavior of the blood flow as the taper of the tube is a vital factor in the pressure development[12]. Thurston[18] was among the earliest to recognize the viscoelastic nature of blood and that the viscoelastic behavior is less prominent with increasing shear rate. Anand et.al.[1] have developed a model that is suitable for blood simulation and it contains Oldroyd-B fluid flow characteristics. Rajagopal and Srinivasa[14] have described a thermodynamic framework which is well suited for describing the viscoelastic response (blood) of bodies with multiple configurations. To captures the shear-thinning rheological behavior a DA method has developed by D'Elia et. al.[3] to show the numerical simulation of blood flow in 2D idealized stenosis with wall shear stress effect. Numerical simulation of generalized Newtonian and Oldroyd-B fluid have studied by V. Prokop et al.[13] with an extended computational domain. G. Telma et. al.[17] have studied the blood flow simulations can improved by integrating known data in 2D idealized stenosis vessels. Nasir and Alim[20] have studied that numerical study of blood flow through symmetry and non-symmetric stenosis artery under various flow rates. The Numerical modelling of

viscous and viscoelastic fluids flow through the branching channel have discussed by K. Radka et.al.[6]. Recently, M. Mahfoud et.al.[10] have shown that the pulsatile blood flow through an arterial stenosis to evaluate the flow characteristics and the wall shear stress under physiological conditions. In the present work, a numerical investigation of blood flow through stenotic artery have been studied. The governing mass, momentum and Oldroyd-B equation are expressed in a normalized primitive variables formulation. In this thesis, a finite element method for steady-state incompressible blood flows has been developed.

Model Specifications

In this study, the blood is assumed to be laminar, incompressible, and Newtonian. The physical model considered here is shown in Fig.1, along with the important geometric parameters. The stenosed vessel is assumed to be two-dimensional with diameter D = 2R = 6.2mm which reduces smoothly to one half in the stenosed region. The parabolic velocity profile is prescribed at the inlet and pressure is fixed to a constant at outlet. On the walls, no-slip conditions are used for velocity and homogeneous Neumann condition for the pressure. For Oldroyd-B model variables (σ_v) there is zero kept at the inlet and homogeneous Neumann condition at the walls and at the outlet. The stenosis cross-sectional area ration is 2:1 and thus a significant local acceleration of the flow is expected.

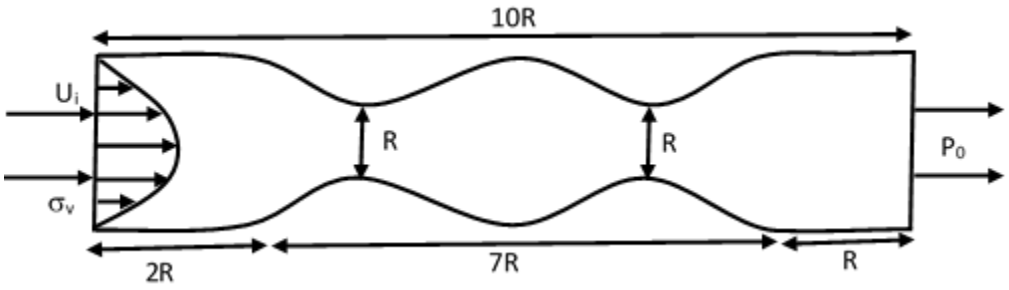

Figure 1: Schematic diagram of the physical system.

Mathematical Model

The present problem is a two dimensional and the blood flow fluid is assumed to be incompressible and steady. A set of coupled, nonlinear, and partial differential equations are continuity, momentum and Oldroyd-B equations for blood flow. We have used non-dimensional scale variables to derive dimensionless equations as follows:

Continuity Equation

$$\nabla . \mathbf{U} = 0 \qquad (1)$$

Momentum Equations

$$\mathrm{Re}[(\mathbf{U}.\nabla)\mathbf{U}] = -\nabla P + (1-\lambda)\Delta\mathbf{U} + \nabla.\boldsymbol{\sigma} + \mathbf{f} \qquad (2)$$

Oldroyd-B constitutive equation:

$$W_i[(\mathbf{U}.\nabla)\boldsymbol{\sigma}] + \boldsymbol{\sigma} = 2\mu_v \mathbf{V}(\mathbf{U}) + W_i[(\nabla\mathbf{U})\boldsymbol{\sigma} + \boldsymbol{\sigma}(\nabla\mathbf{U})^t] \qquad (3)$$

Boundary conditions: The boundary conditions are

At inlet

(i) Dirichlet boundary conditions for velocity vector are used on the boundary $\partial\Omega$.

(ii) For a pressure and the stress tensor Neumann boundary condition is used on the boundary$\partial\Omega$.

(iii)The developed parabolic velocity profile and the corresponding extra stresses components.

$$u = 1.5\,(1-s^2),\ v = 0, \sigma_{11} = 2\mu_v Wi\left(\frac{\partial u}{\partial y}\right)^2,\ \sigma_{12} = \mu_v \frac{\partial u}{\partial y} \text{ and } \boldsymbol{\sigma}_{22} = 0$$

At outlet

(i) At outflow boundary pressure value is constant and for the velocity vector and the stress tensor Neumann boundary condition is used.

(ii) Due to pressure force (P_o) the stress is acting at the boundary $\mathbf{T}.\mathbf{n} = -P_o\mathbf{n}$.

At Boundary Wall

(i) On the walls, no slip conditions are used for the velocity together with the condition for the normal component of the extra stress: $\mathbf{u} = 0$ and $(\mathbf{T}.\mathbf{n}).\mathbf{n} = 0$ Where n is the boundary unit normal vector.

(ii) Homogenous Neumann boundary conditions are used for the pressure.

The above equations were normalized using the following dimensionless scales:
$x=LX$, $t = Lt^*/U$, $u = UU_o$, $\mathbf{v} = VU_o$, $p = \mu UP/L$, $T = U\mu T^*/L$, $f = f^*\mu U/L^2$, $\nabla=\nabla^*/L$, $Wi = \lambda_x U/L$, $Re = \rho UL/\mu$, where Reynolds number (Re) and Weissenberg number (Wi) are dimensionless numbers. Small values of Wi mean that the fluid is little elastic and small values of Re means that the fluid is very viscous.

Numerical Analysis

To solve the continuity, momentum and Oldroyd-B equations numerically, we have used Galergkin weighted residual finite techniques, MATLAB Programming[7] and the commercial

high-level finite element package COMSOL Multiphysics[2]. The application of this technique is well described by Taylor and Hood[16] and Dechaumphai[4,5]. The finite element method and computational technique have been omitted here for brevity.

Grid Independence Test

To decide the suitable grid size for this study, a grid independence test is performed with *Re* = 10^2 and Wi = 0.6, μ_0 = 0.16 Pa.s, μ_n = 0.0036 Pa.s, a = 1.23,b = 0.64,λ = 8.2s, ρ = 1050 kg.m-3, L_w = 0.003m and L= 0.03m. and blood flow rate 0.1cm^3/s. Figure 2 shows the convergence of the average velocity (U) along the vessel axis with grid refinement. It is observed that grid independence is achieved with 22585 elements where there is insignificant change in velocity with further increase of mesh elements. Six different non-uniform grids with the following number of nodes and elements were considered for the grid refinement tests: 28442 nodes, 7355 elements; 50346 nodes, 9500 elements; 64240 nodes, 12586 elements; 69887 nodes, 14371 elements; 92573 nodes, 22585 elements, 98388 nodes, 29686 elements. From these values, 92573 nodes, 22585 elements can be chosen throughout the simulation to optimize the relation between the accuracy required and the computing time.

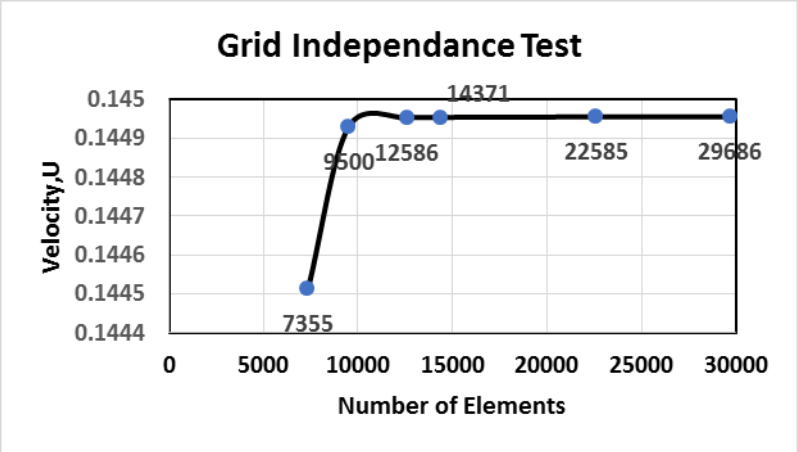

Figure 2: Convergence of average velocity with grid refinement for *Re* = 10^2 and Wi = 0.6 with blood flow rate 0.2cm^3/s.

RESULT AND DISCUSSION

The aim of the present model is to identify and show the effects of stenosis, wall shear stenosis, dimensionless numbers and various flow rate on blood flow for the Newtonian (N), generalized Newtonian (GN), Oldroyd-B (OD) and generalized Oldroyd-B (GD) models. We have investigated the influence of the viscoelastic effects and shear-thinning behavior of blood at various flow situations. The solution of the Navier-Stoke equations is obtained under

the same conditions as the solutions of the non-Newtonian equations. The comparison of blood flow field is presented to show the non-Newtonian effects. To developed models, the only change of blood viscosity μ_n and extra stress T_v is consider. The blood flow simulations and investigation have performed and compared for all four models. The following parameters[8] have been used for blood flow simulations in aorta μ_0 = 0.16 Pa.s, μ_n = 0.0036 Pa.s, a = 1.23,b = 0.64,λ = 8.2s, ρ = 1050 kg.m-3, L_w = 0.003m and L= 0.03m. To code validation, the blood flow simulation with above mentioned parameters for Newtonian model have solved, and the results have compared with those reported by V. Prokop et al.[13], obtained with an extended computational domain. A comparison between the simulation of blood velocity contour lines are presented. The results from the present experiment are almost same as V. Prokop et al.

V. Prokop et al. (2013)	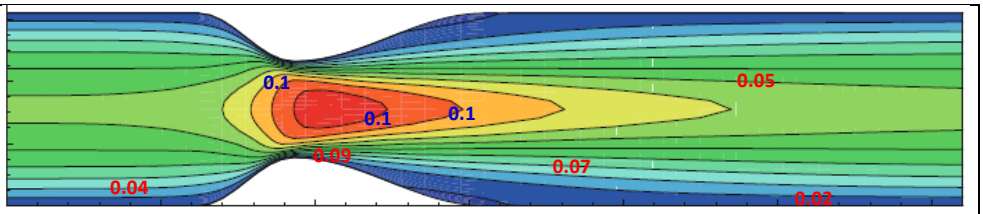
Present Work	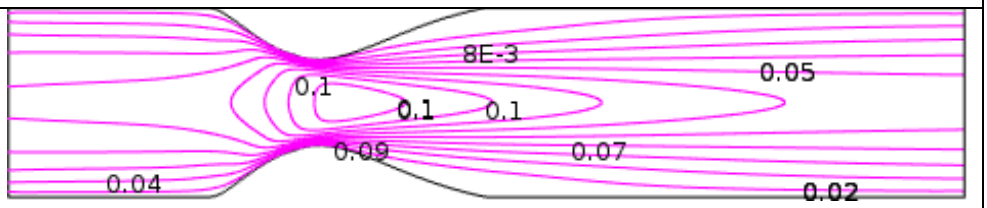

Figure 3: Comparison of velocity contour of blood flow through stenotic artery.

Stenosis Effects on blood flow characteristics

The blood flow characteristics of the Newtonian, Generalized Newtonian, Oldroyd-B, Generalized Oldroyd-B models are presented in fig. 4 at the flow rate q=0.2 cm^3/s. The blood flow characteristics (axial velocity contours and pressure distribution) have a significant changed at throat of stenosis. There are some permanent recirculation zone or flow separation zone formed at stenosis. These recirculation zones are indicative of regions where the flow is reversed over a significant portion of each model. At generalized Newtonian and Oldroyd-B model, the recirculation zone becomes slight shorter than other models. It is also observable that the reversal flow regions and flow separation are found at just behind the stenosis with respect to the centerline. In blood flow experiments blood pressure can easily be measured, the pressure drops (i.e. the inlet-outlet pressure difference) needed to achieve a prescribed flow rate. At fig. 5, some parabolic pressure profile has developed and similarities are found

at far from the stenosis of the artery. While the axial pressure profiles are pronounced at the around of first stenosis and some departures from the parabolic profile at second stenosis, because of great shear acting on the fluid in these regions. The intensive pressure gradient is found at stenosis area but relatively steep pressure contours are obtained at the far the constriction regions.

The axial velocity profiles and pressure profile are shown in fig. 6 and 7 for all four models at dimensionless number Wi=0.6 and Re=100. Form the fig. 6, the minimum value of velocity is found in 1st constriction regions and the lowest value of pressure is found in second stenosis region in fig. 7. It is clearly visible that the main effect of the blood shear-thinning behavior is noticeable in the recirculation zone, where the resistance to flow (local viscosity) increases substantially. The effects of viscoelasticity are about one order of magnitude lower in this case. For pulsatile flow or other flow rates or geometries, the viscoelastic effects may become more vital. The pressure is more dominated at stenosis regions because of the shear-thinning behavior of blood viscosity. It implies that, the flow is quicker than the non-Newtonian ones and its patterns remain in a disturbed state compare to others. The shear-thinning viscosity function leads to the growth of the local viscosity in the low-shear regions at the Newtonian case. In fig. 7, the more negative values are found in the second stenosis region for generalized Newtonian and Oldroyd-B model which leads to non-Newtonian fluid is slower than Newtonian fluid.

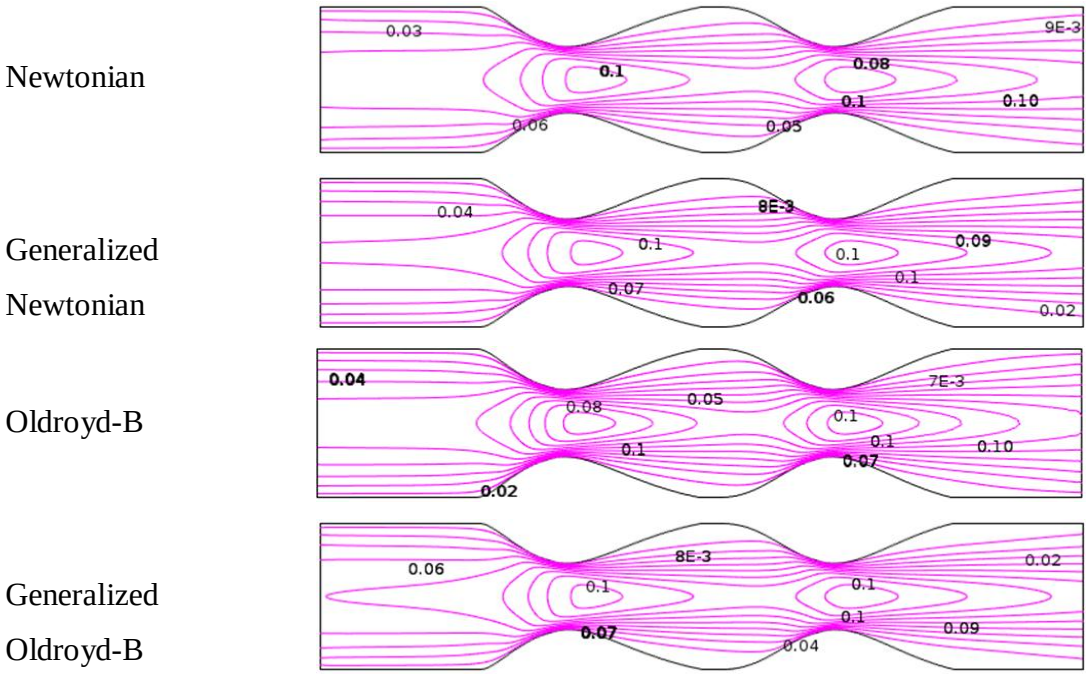

Figure 4: Velocity distribution on blood flow through Symmetric Stenosis at *Re*=100 and *Wi* = 0.6.

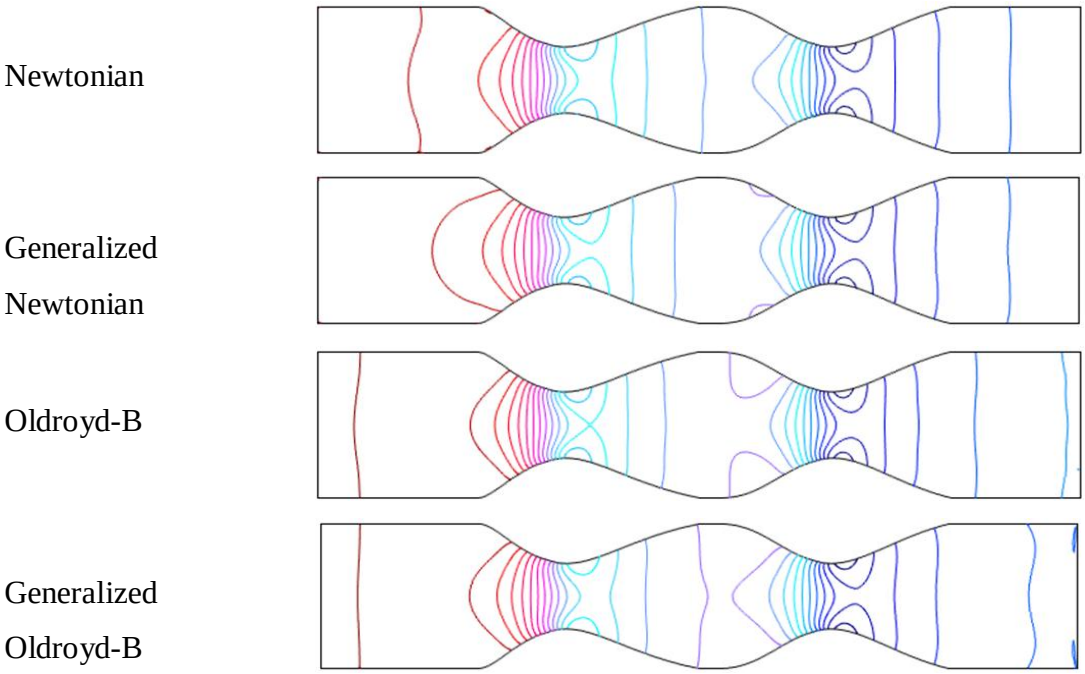

Figure 5: Pressure distribution on blood flow through Symmetric Stenosis at *Re*=100 and *Wi* = 0.6.

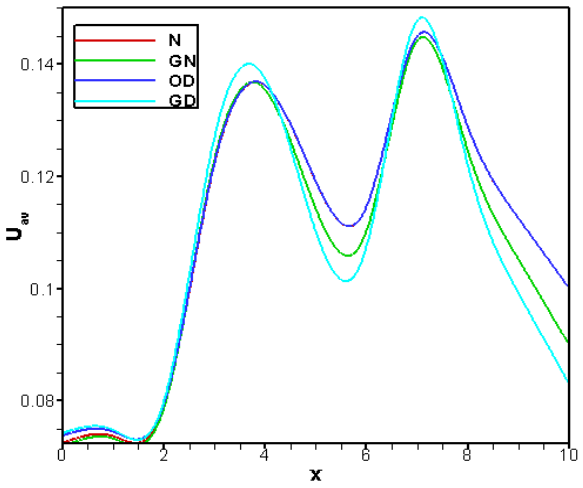

Figure 6: Effect of velocity profile of blood flow along vessel axis.

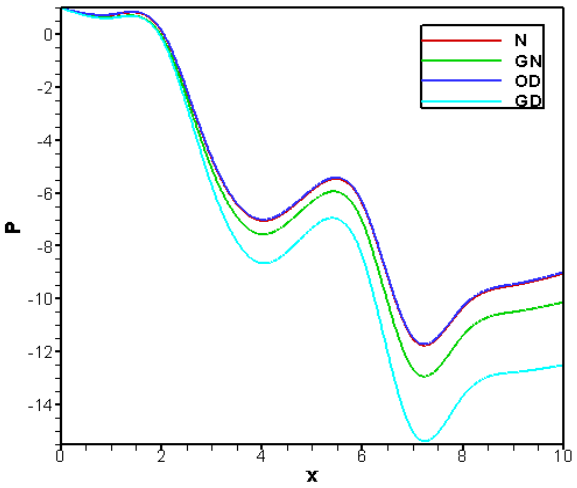

Figure 7: Effect of pressure profile of blood flow along vessel axis.

Dimensionless Numbers effects on blood flow

Reynold Numbers (Re) Effects

The Blood flow patterns affected by different Reynold numbers, *Re* (100, 500 and 1000) and Weissenberg numbers, *Wi* (0.0, 0.5, 1.0) are shown in figs. 8-27 for all four models. It is seen that fluid developed parabolic profile at stenosis area in artery with the increases of *Re* and the pattern of blood flow for velocity and pressure distribution in terms of contour lines are shown in figure 8 to 27. For all models, the graphical representation of the average velocity

and pressure variation for different Reynold numbers, *Re* = 100, 500 and 1000 with flow rate 0.2 cm^3/s are shown in fig. 16 and 17. From these figure, we observe that average velocity speed up around stenosis area with the increases of Reynold numbers and it obtained peak value at second stenosis for all four models because of the effect of inertia. The velocity profile cross each other between the stenosis for a little turbulence blood flow. In fig. 17, we also see that pressure distribution decrease along vessel axis with increases of Reynold numbers, *Re*. The lowest value of pressure is obtained at second stenosis for generalized Oldroyd-B model. In the case of generalized Oldroyd-B, pressure contour lines becoming close each other because of blood shear-thinning behavior.

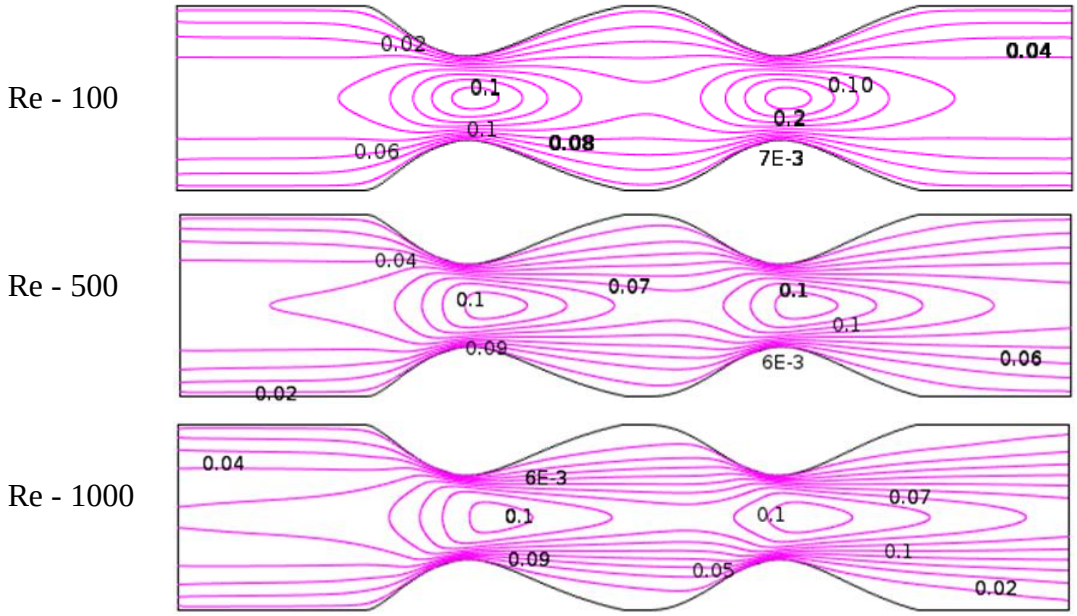

Figure 8: Renylod Numbers (*Re*) effects on Blood flow of Newtonian Model at *Wi* = 0.6 and flow rate 0.2 cm^3/s.

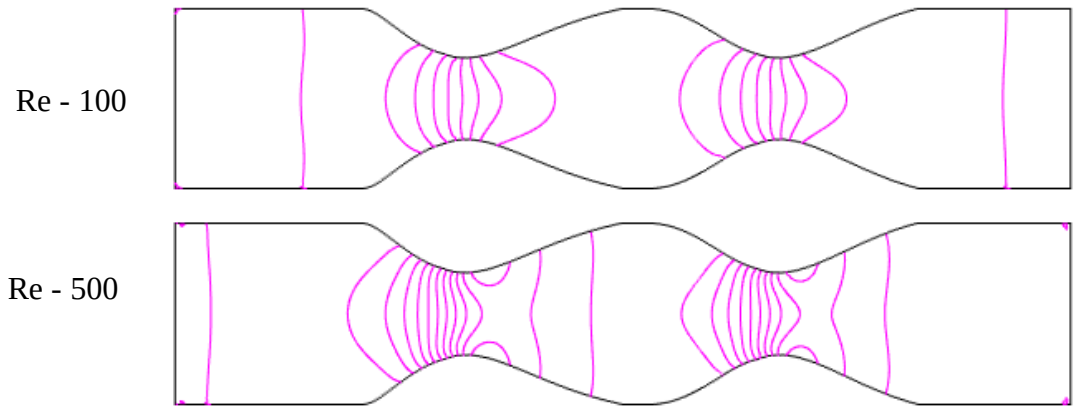

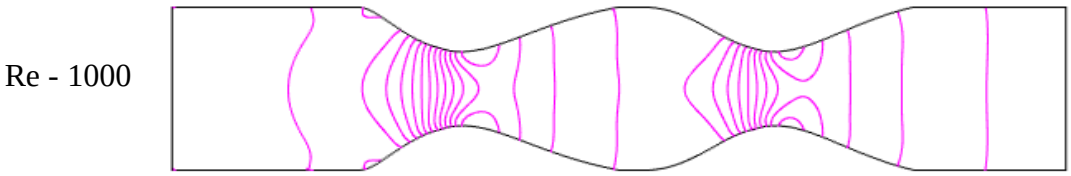

Figure 9: Renylod Numbers (*Re*) effects on pressure distribution of Blood flow for Newtonian Model at *Wi* = 0.6 and flow rate 0.2 cm^3/s.

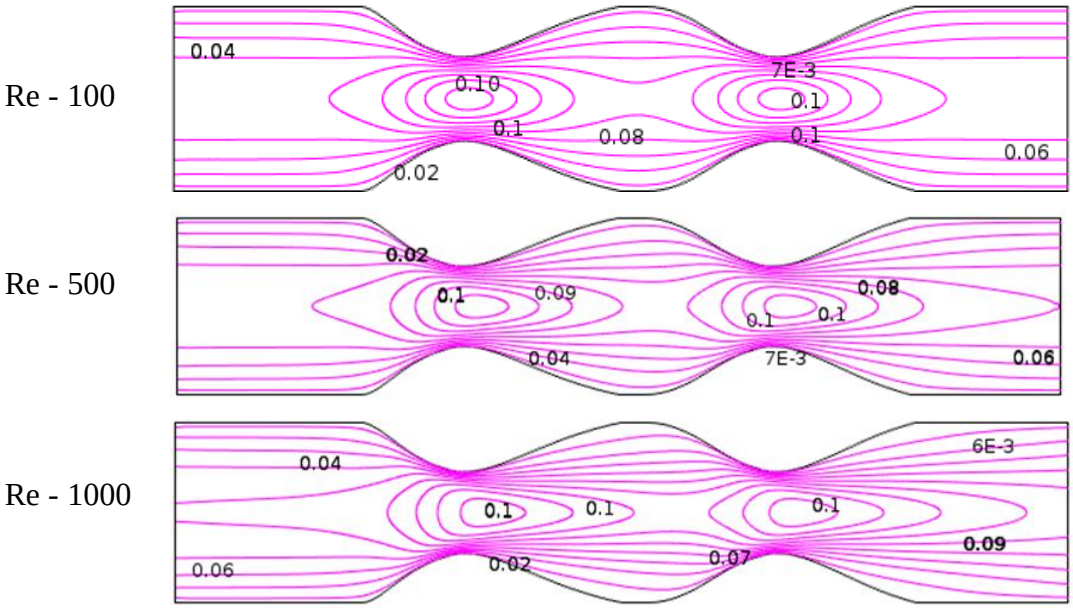

Figure 10: Renylod Numbers (*Re*) effects on Blood flow of Generalized Newtonian Model at *Wi* = 0.6 and flow rate 0.2 cm^3/s.

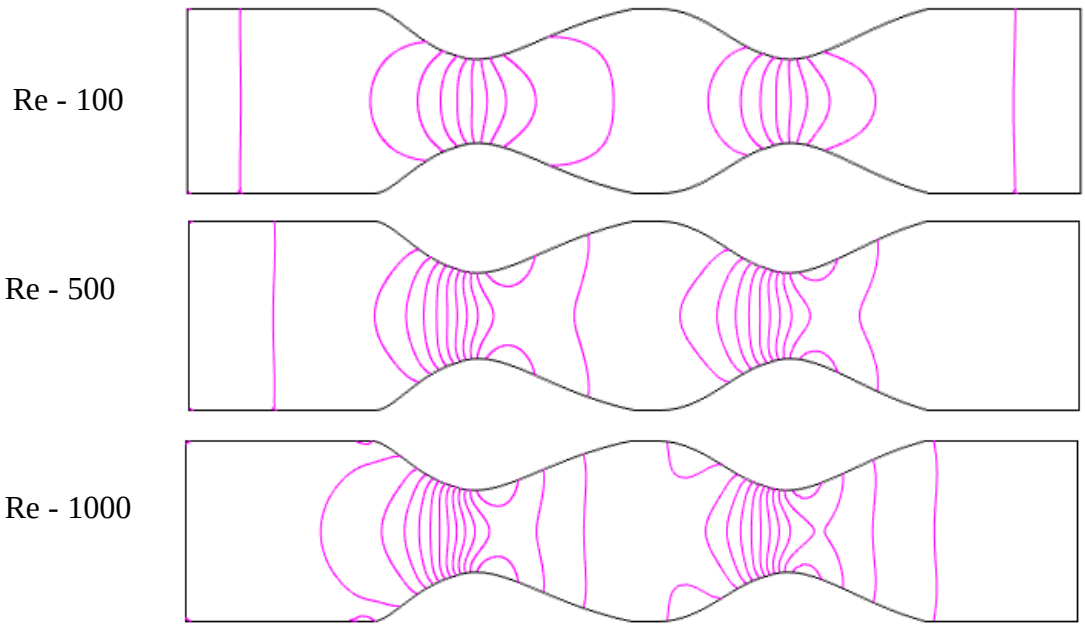

Figure 11: Renylod Numbers (Re) effects on pressure distribution of Blood flow for Generalized Newtonian Model at Wi = 0.6 and flow rate 0.2 cm^3/s.

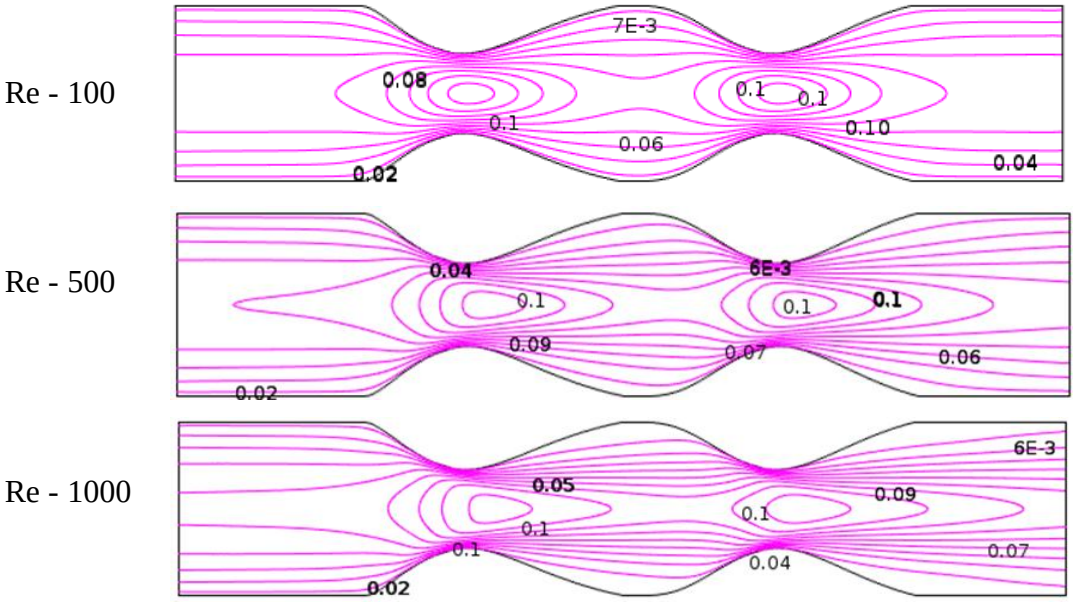

Figure 12: Renylod Numbers (Re) effects on Blood flow of Oldroyd-B Model at Wi = 0.6 and flow rate 0.2 cm^3/s.

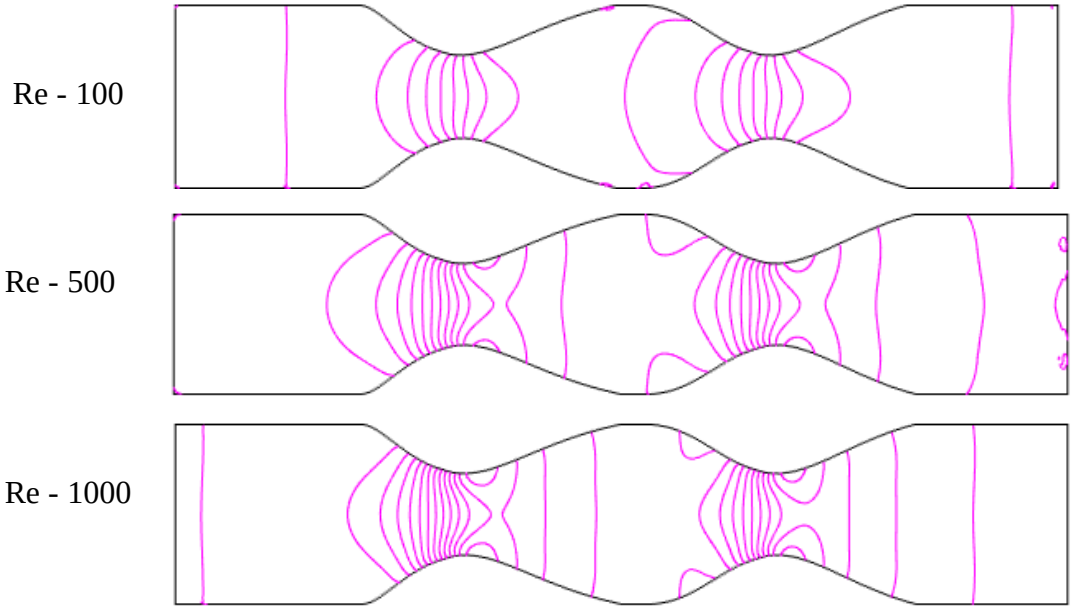

Figure 13: Renylod Numbers (Re) effects on pressure distribution of Blood flow for Oldroyd-B Model at Wi = 0.6 and flow rate 0.2 cm^3/s.

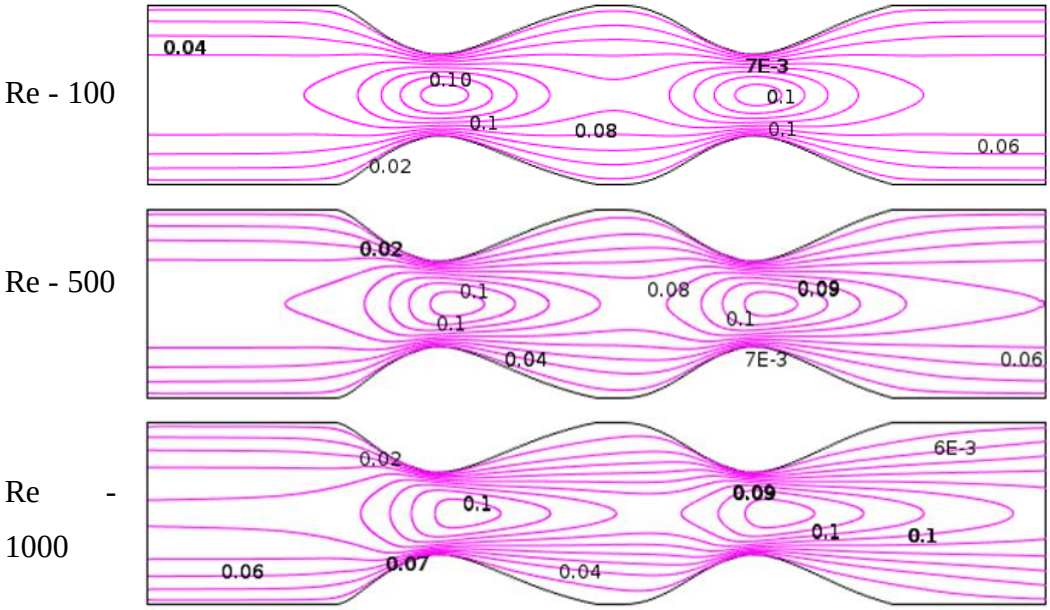

Figure 14: Renylod Numbers (Re) effects on Blood flow of Generalized Oldroyd-B Model at Wi = 0.6 and flow rate 0.2 cm^3/s.

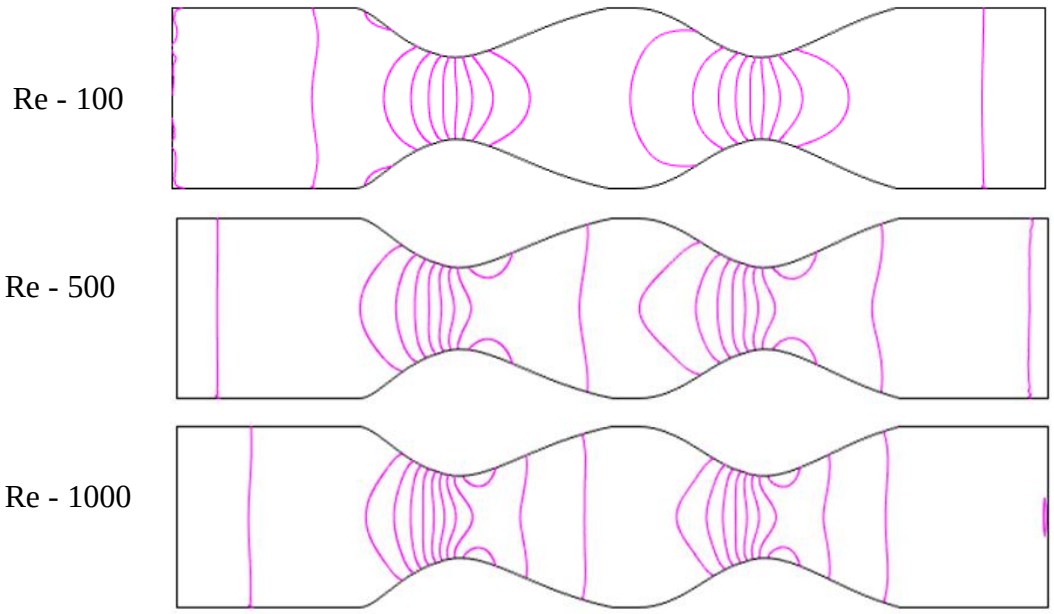

Figure 15: Renylod Numbers (Re) effects on pressure distribution of Blood flow for Generalized Oldroyd-B Model at Wi = 0.6 and flow rate 0.2 cm^3/s.

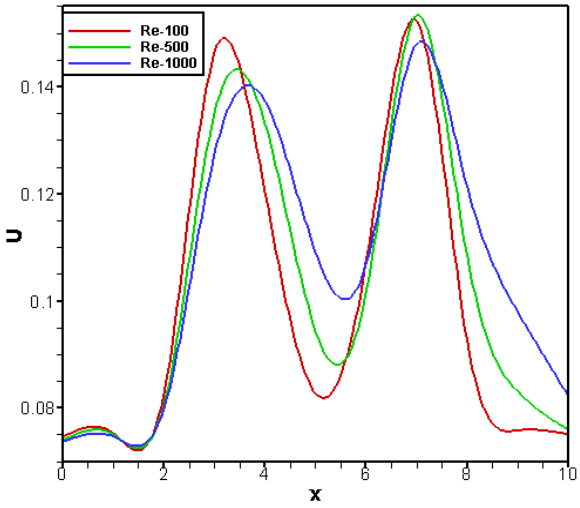

Fig 16a

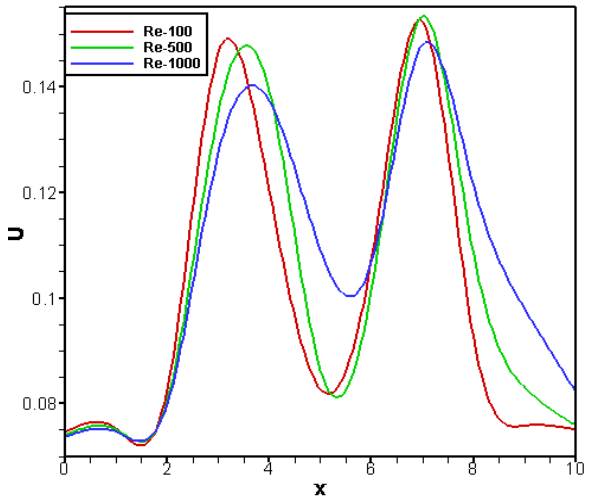

Fig 16b

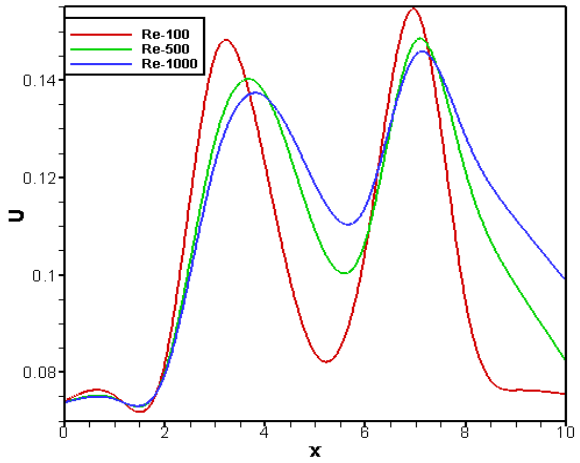

Fig 16c

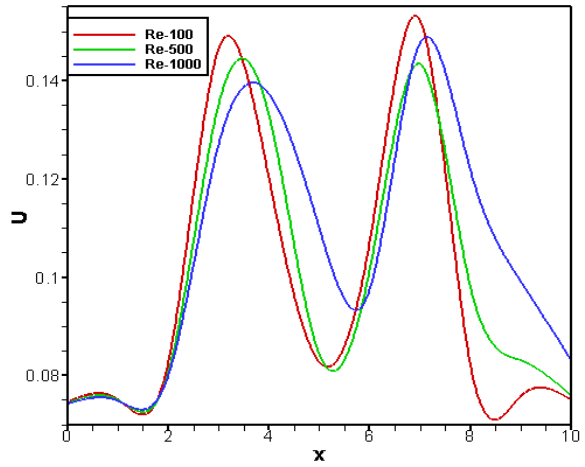

Fig 16d

Fig 16: Velocity profile of various Re on Blood flow at Wi = 0.6 for (16a) Newtonian, (16b) Generalized Newtonian, (16c) Oldroyd-B and (16d) Generalized Oldroyd-B Model.

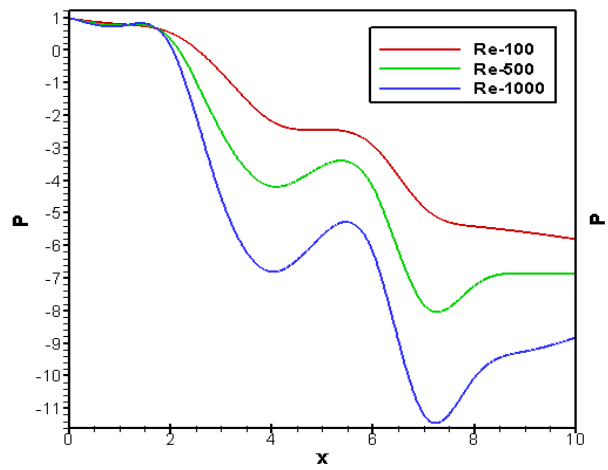

Fig 17a

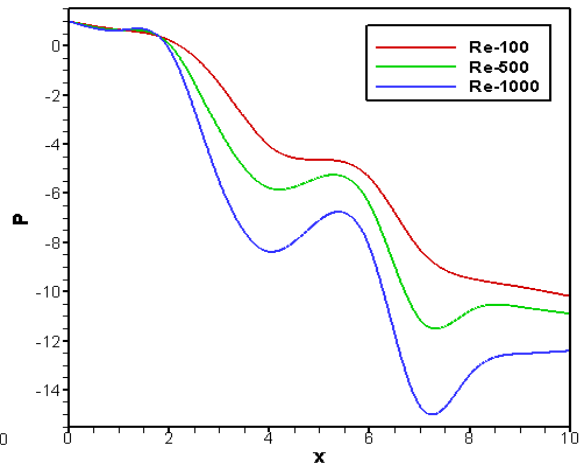

Fig 17b

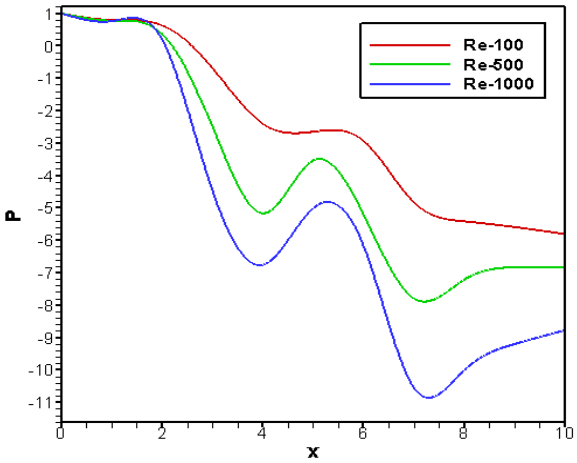

Fig 17c

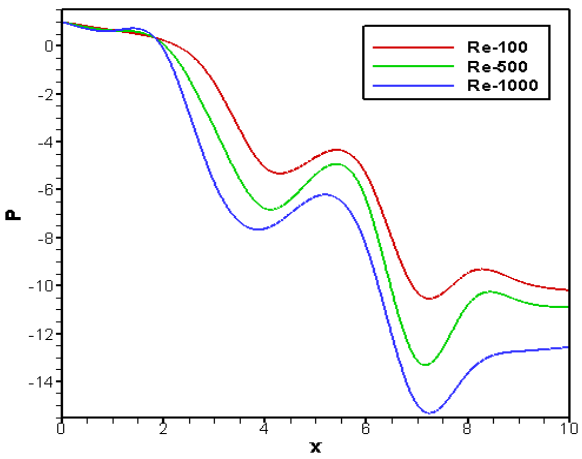

Fig 17d

Fig 17: Pressure profile of various Re on Blood flow at Wi = 0.6 for (Fig 17a) Newtonian, (Fig 17b) Generalized Newtonian, (Fig 17c) Oldroyd-B and (Fig 17d) Generalized Oldroyd-B.

Weissenberg Numbers (Wi) Effects

Again, the effects of Weissenberg numbers, *Wi* (0.0, 0.5, 1.0) on blood flow are shown in figs. 18-27 for all four models with the flow rate at *Re* = 100. At Wi=0.0 leads that the fluid is pure viscous fluid i.e. no elasticity while an infinite Weissenberg numbers limit corresponds to purely elastic response. At Wi = 0.0, we have found small vortex for all models. Since at low shear rate, blood aggregate are solid-like bodies, and has ability to store elastic energy. We observe that velocity increases at the stenosis throat with the increases of *Wi* and create big vortex at second constriction for *Wi*=1.0. Due to less dominant of viscous force the velocity is higher at *Wi* =1.0 which leads to bigger vortex and blood behave fluid-like bodies. At *Wi* =0.5, a small recirculation has found at stenosis and just after stenosis velocity fall down and create a back flow adjacent to vessel wall. In fig. 26, we attained maximum value of velocity at center of stenosis for all four models and have little different at beginning. The pressure is more dominated at the constriction area of the stenosis cavity for all models. At stenosis regions pressure is lower than other region because of the shear-thinning characteristics of blood viscosity which leads the flow is faster than the non-Newtonian ones and its patterns remain in a disturbed state compare to others. From the figure 27, the minimum value of pressure is found at second stenosis area and pressure profile are almost similar at generalized Oldroyd-B model. In fig. 27, the numerical values of pressure distribution are presented for all the four models Newtonian, Generalized Newtonian, Oldroyd-B, Generalized Oldroyd-B with the flow rate q=0.2 cm^3/s.

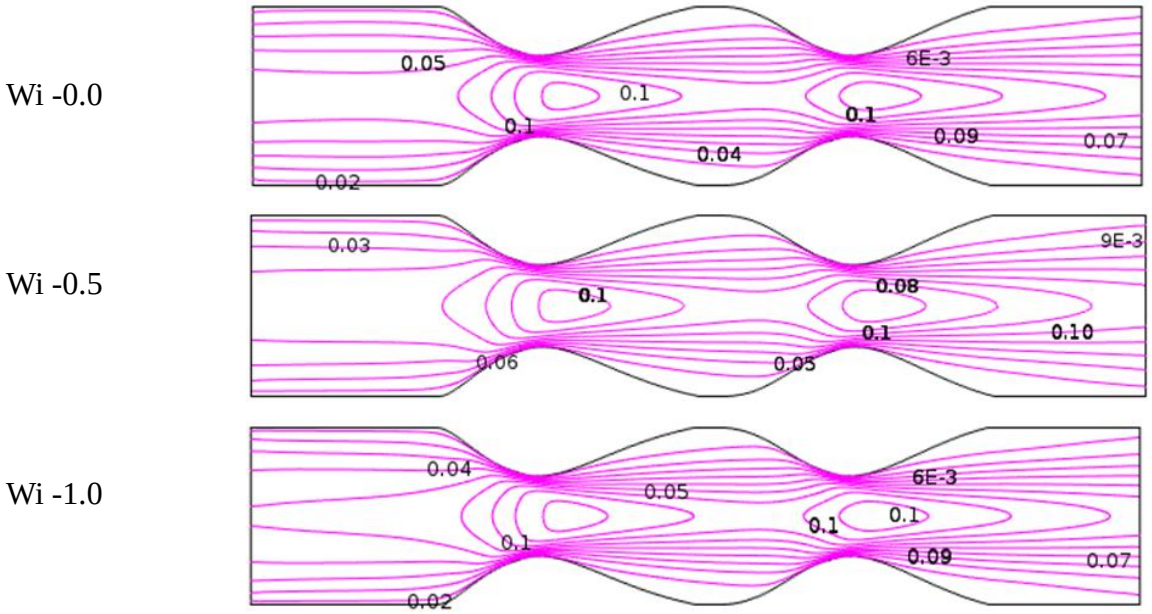

Fig 18: Weissenberg Numbers (Wi) effects on Blood flow of Newtonian Model at Re = 100 and flow rate 0.2 cm^3/s.

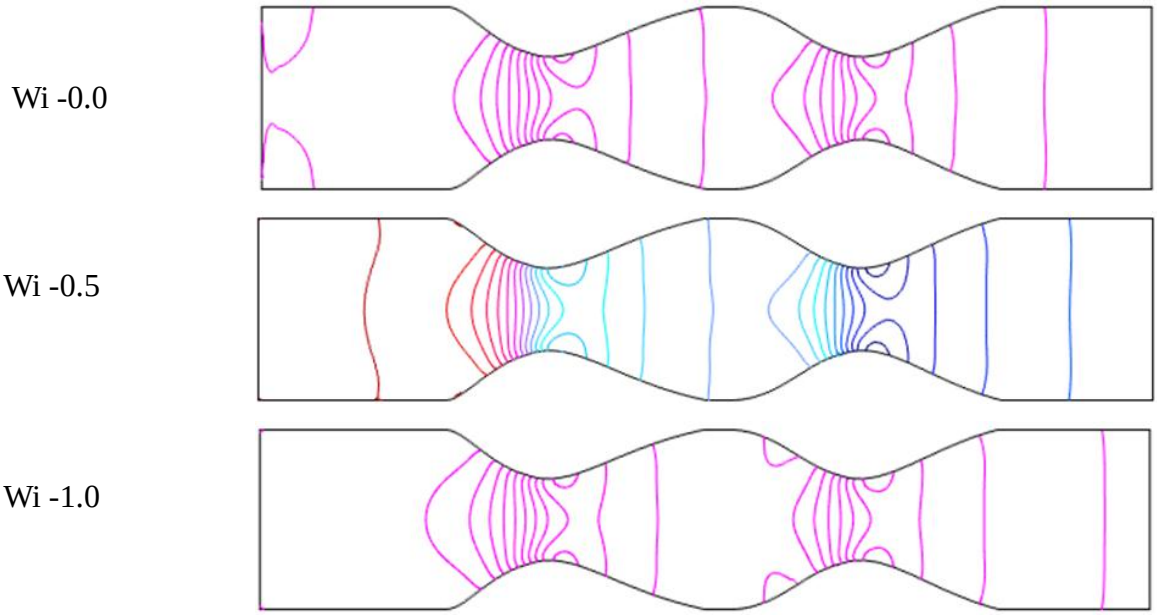

Fig 19: Weissenberg Numbers (Wi) effects on pressure distribution of Blood flow for Newtonian Model at Re = 100 and flow rate 0.2 cm^3/s.

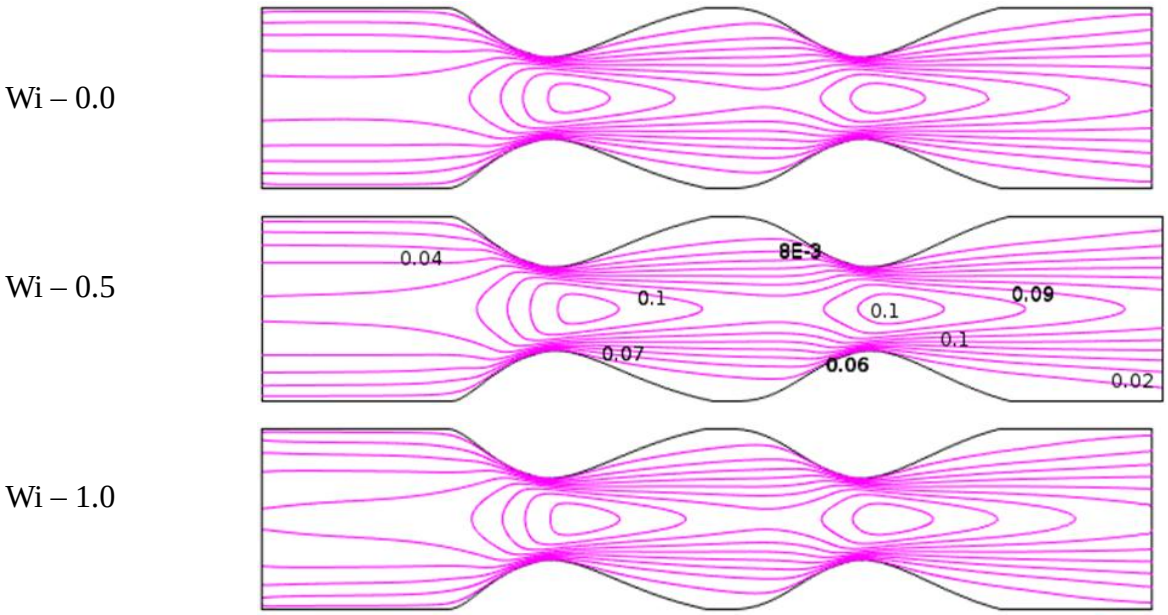

Fig 20: Weissenberg Numbers (Wi) effects on velocity distribution of Blood flow for Generalized Newtonian Model at Re = 100 and flow rate 0.2 cm^3/s.

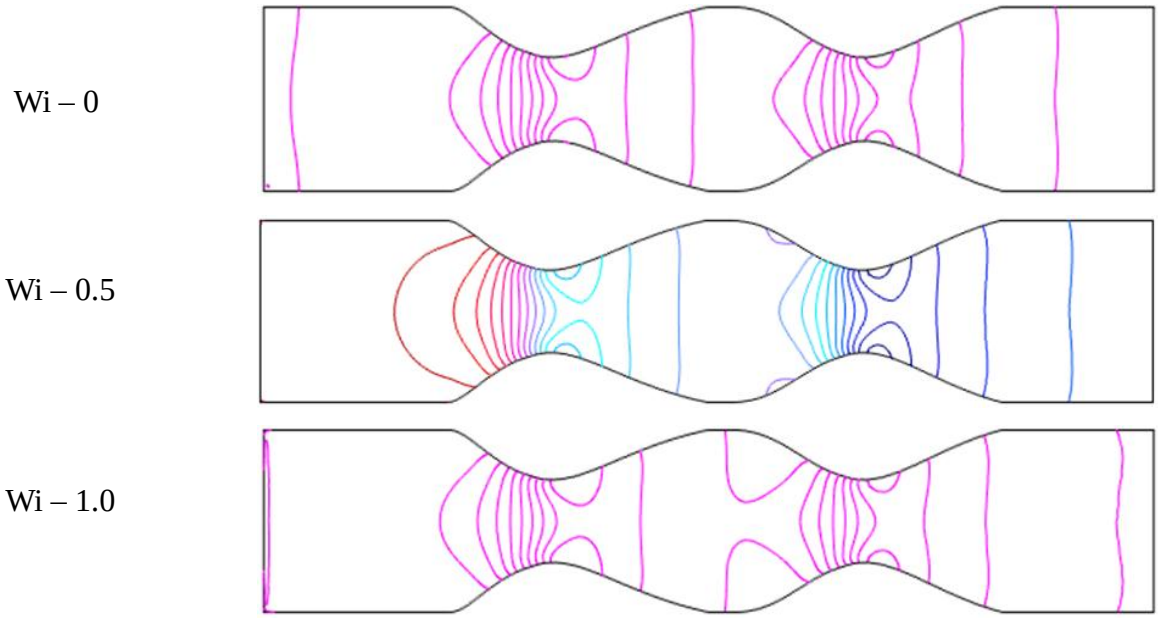

Fig 21: Weissenberg Numbers (Wi) effects on pressure distribution of Blood flow for Generalized Newtonian Model at Re = 100 and flow rate 0.2 cm^3/s.

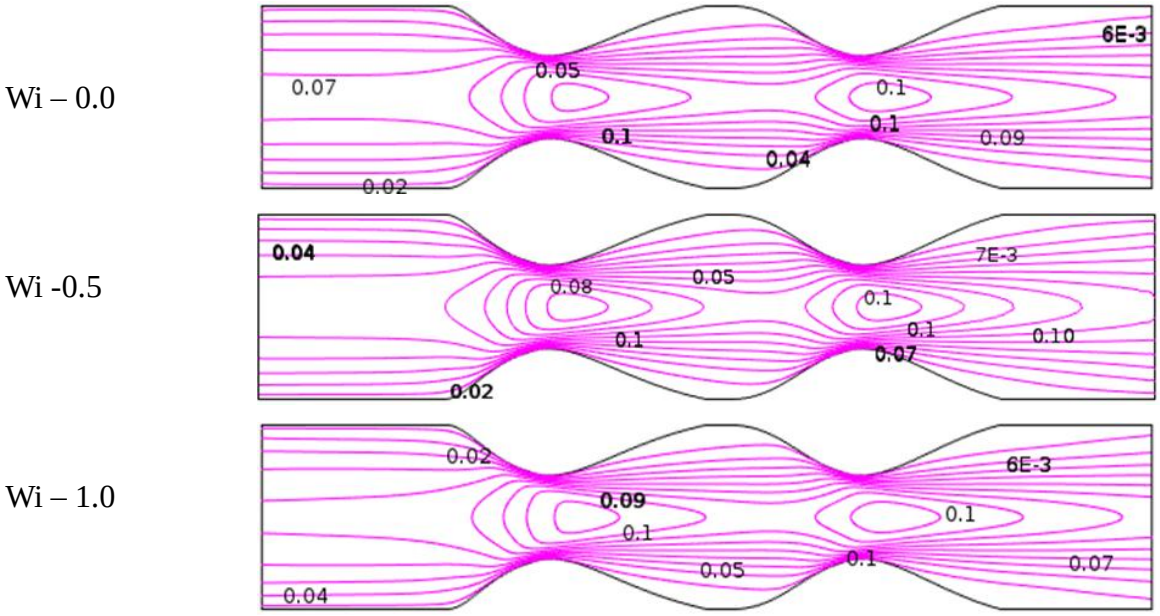

Fig 22: Weissenberg Numbers (Wi) effects on velocity distribution of Blood flow for Oldroyd-B Model at Re = 100 and flow rate 0.2 cm^3/s.

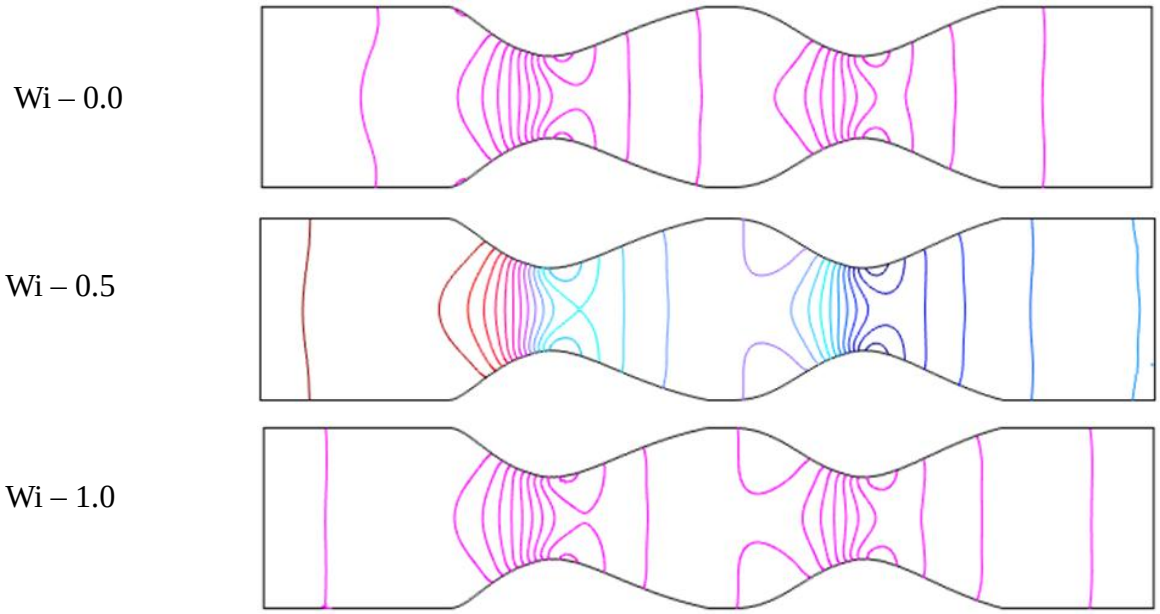

Fig 23: Weissenberg Numbers (Wi) effects on pressure distribution of Blood flow for Oldroyd-B Model at Re = 100 and flow rate 0.2 cm^3/s.

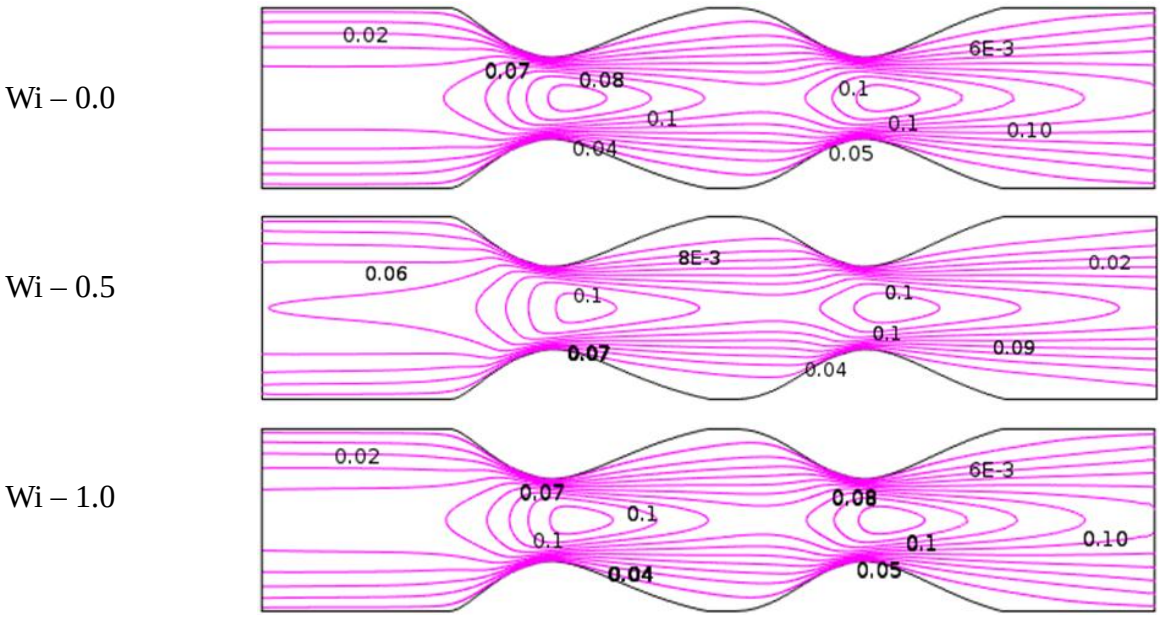

Fig 24: Weissenberg Numbers (Wi) effects on Velocity distribution of Blood flow for Generalized Oldroyd-B Model at Wi = 0.6 and flow rate 0.2 cm^3/s.

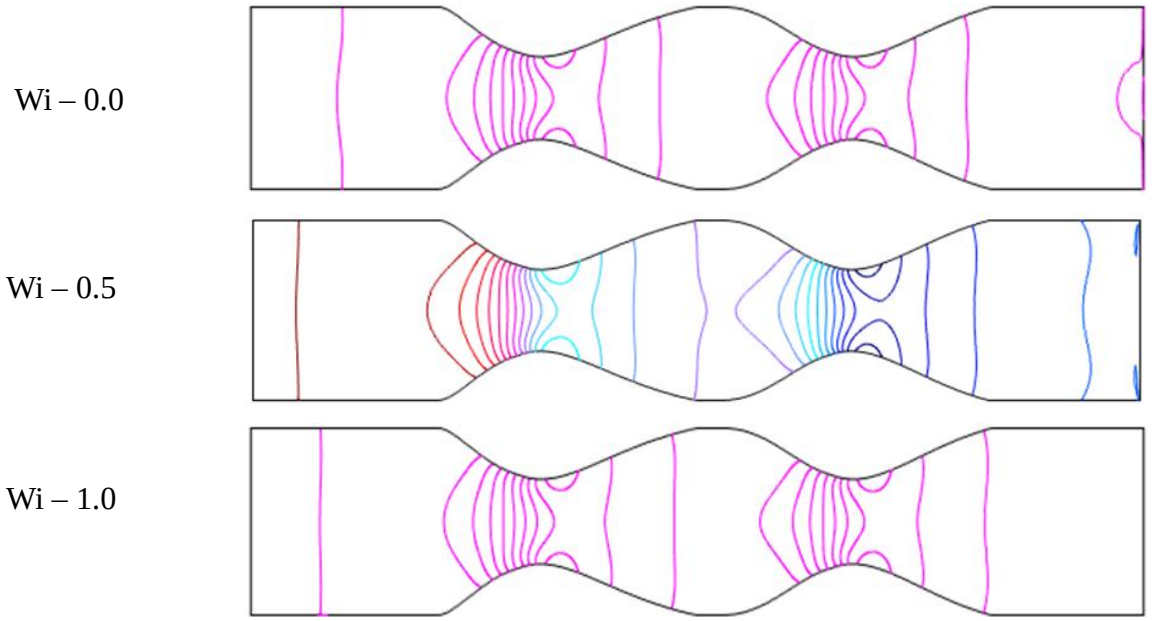

Fig 25: Weissenberg Numbers (Wi) effects on pressure distribution of Blood flow for Generalized Oldroyd-B Model at Wi = 0.6 and flow rate 0.2 cm^3/s.

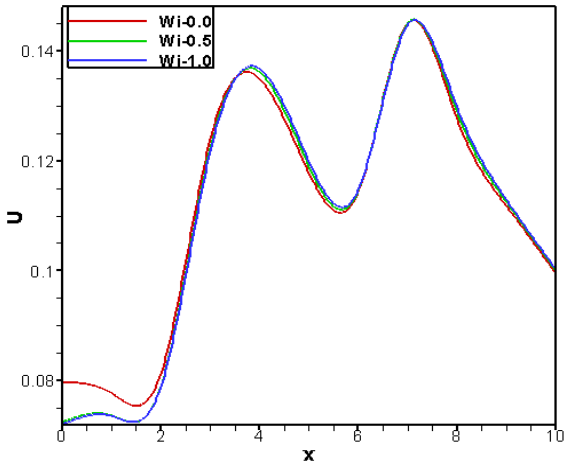

Fig 26a

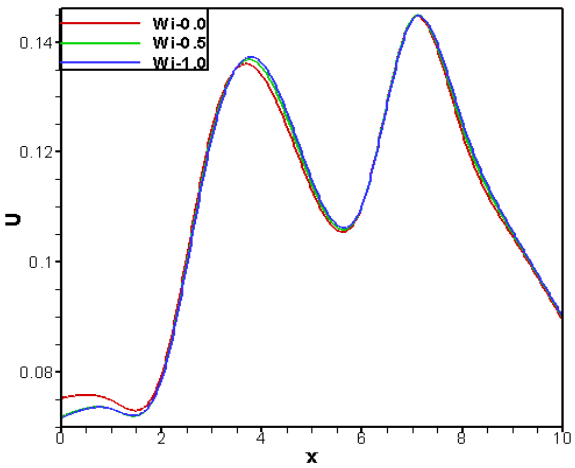

Fig 26b

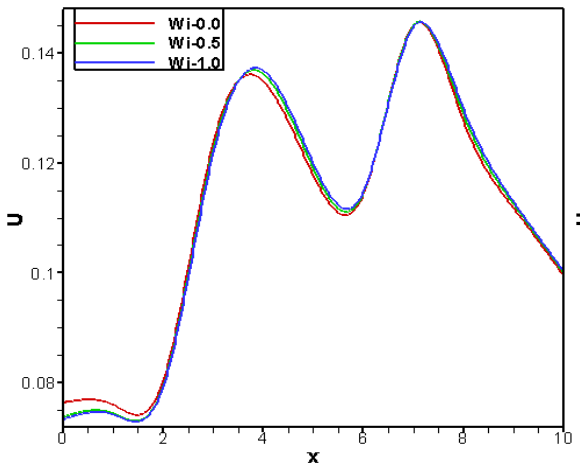

Fig 26c

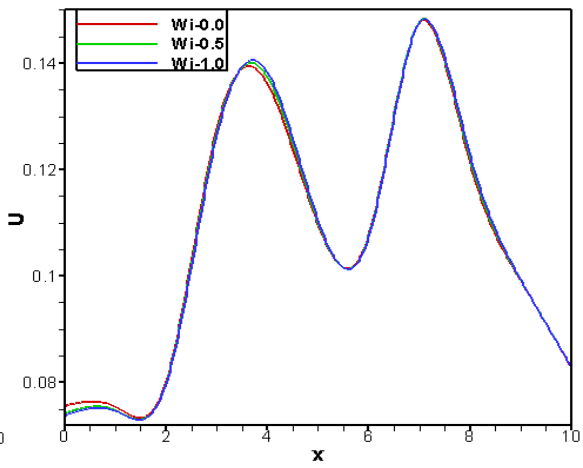

Fig 26d

Fig 26: Velocity profile of the Effect of Reynold numbers (Re) on Blood flow at Wi = 0.6 and flow rate 0.2 cm^3/s for (26a) Newtonian Model, (26b) Generalized Newtonian Model, (26c) Oldroyd-B Model, and (26d) Generalized Oldroyd-B Model.

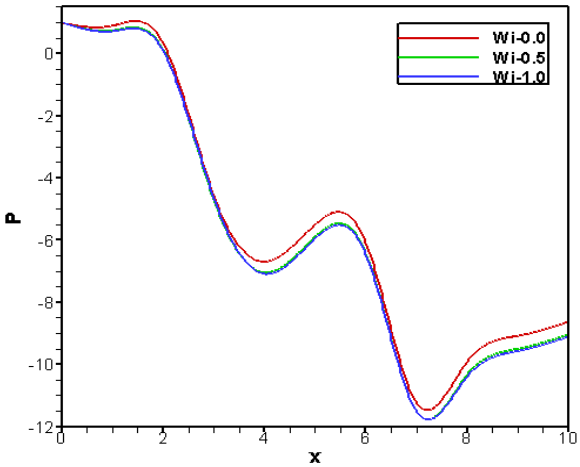

Fig 27a

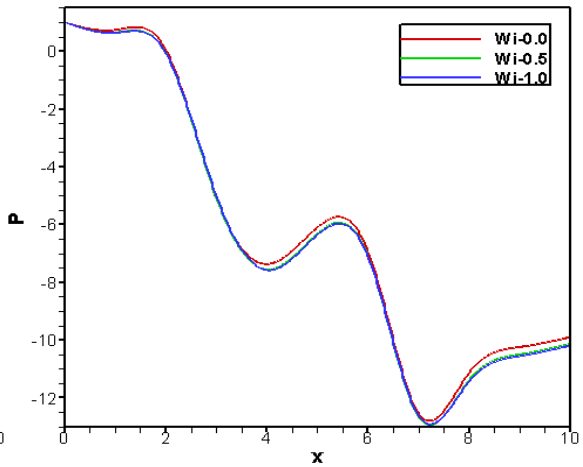

Fig 27b

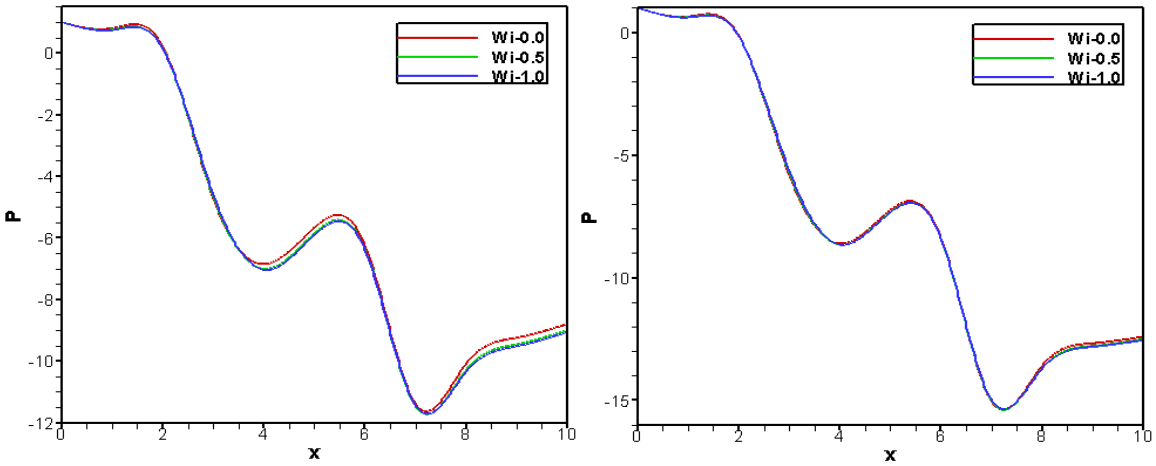

Fig 27c **Fig 27d**

Fig. 27: Pressure profile of the Effects of Weissenbegr numbers (Re) on Blood flow at Re = 100 and flow rate 0.2 cm^3/s for (Fig 27a) Newtonian Model, (Fig 27b) Generalized Newtonian Model, (Fig 27c) Oldroyd-B Model, and (Fig 27d) Generalized Oldroyd-B Model.

Various Flow rates on Blood flow

The blood flow behavior are shown in figs. 28 and 29 with various flow rates for all cases. It is clear that the figure the blood shear -thinning behavior is more intensified at stenosis area compare to non-stenosis. The velocity is slight lower for generalized Oldroyd-B model compare to other models. At flow rate 5 cm^3/s, the Newtonian and Oldroyd-B model very close and same result for rest of two models. On the other hand, the pressure distribution along vessel axis are presented in fig. 29 with different flow rates. The pressure is decreased with respect to vessel axis for all four models. At second stenosis, we obtained lowest value of pressure. For higher flow rate, the pressure profile almost same for all models.

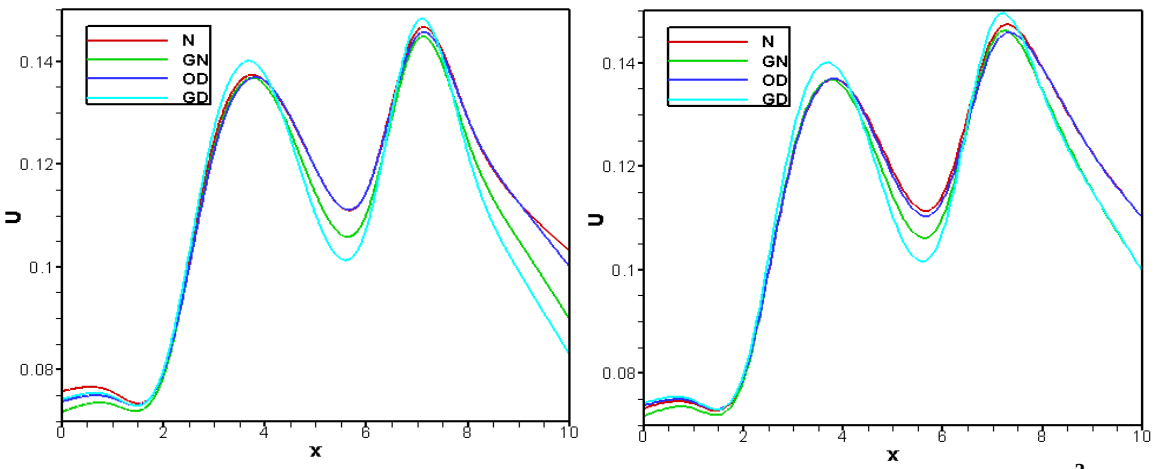

Figure 28: Velocity profile on Blood flow with various flow rate (i) q = 0.01 cm^3/s (left) and (ii) q = 5 cm^3/s (right) at *Wi* = 0.6 and *Re*= 100.

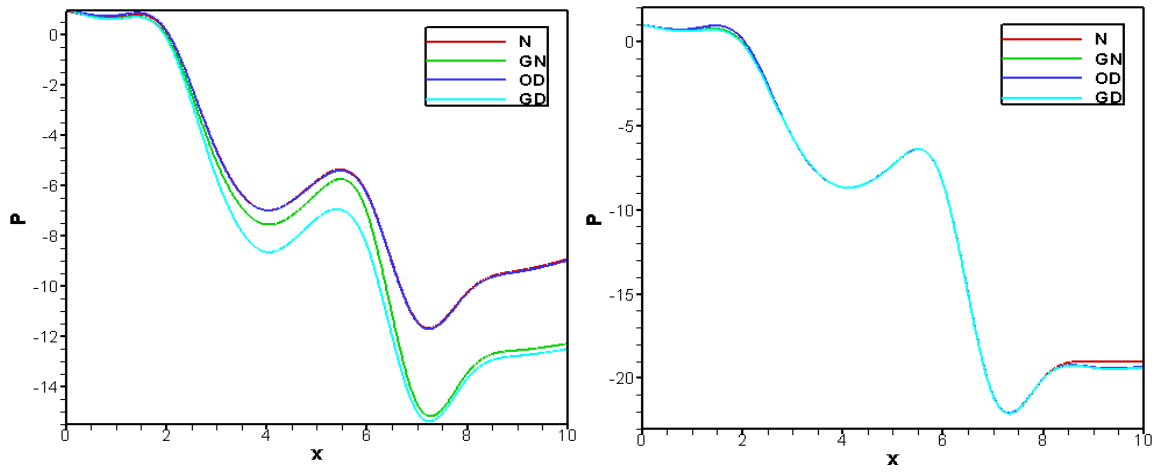

Fig. 29: Pressure profile on Blood flow with various flow rate at *Wi* = 0.6 and *Re*= 100.

Wall Shear Stress effects

The effect of the blood flow behaviour on the wall shear stress is a significant factor in the onset of arterial diseases. In figure 30, show the variation of the wall shear stress for the four models Newtonian, Generalized Newtonian, Oldroyd-B, Generalized Oldroyd-B with the flow rate q=0.2 cm^3/s. The wall shear stress (Wss) is another vital parameter in blood flow simulation. It represents the tangential component of the surface force at the vessel wall, acting against the fluid flow and can define as follows

$$\mathbf{W_{ss}} := -(\mathbf{T}.\mathbf{n}).\mathbf{t}$$

Here **n** is the local wall normal vector (pointing towards the fluid) and **t** is the corresponding unit tangential vector. The wall shear stress profiles for all the models at Wi = 0.6 and Re = 100 are shown in fig. 30. At stenosis region, the negative values are found and flow speeds up significantly in another region in artery. It if found that the wall shear stress increases gradually within axis length 0 to 1.8 and decreases rapidly within 1.8 to 3. It then increases within 3 to 4.5 then it decreases along axis 4.5 to 6.1 and so on. The wall shear stress of generalized Newtonian and Oldroyd-B model is marginally lower than the others model and the wall shear stress of generalized Oldroyd-B model is significantly lower than other models.

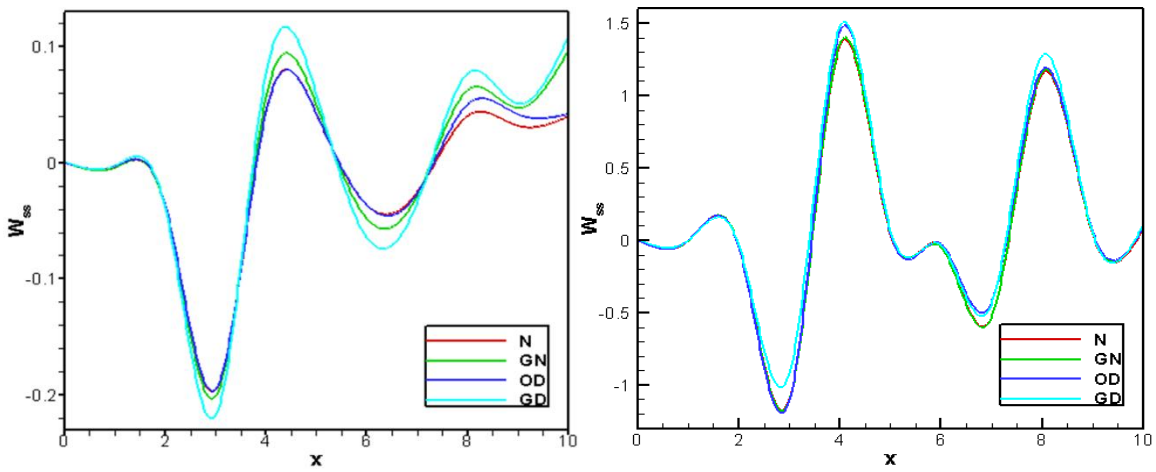

Figure 30: Effects of wall shear stress on blood flow through symmetric stenosis at Re=100 and Wi = 0.6 with various flow rate q = 0.05(left) and 2 (right) cm^3/s.

CONCLUSION

The finite element technique has used to simulate the blood flow through wavy stenosis artery for Newtonian, Oldroyd-B and their generalized models. The numerical investigation of all four models have been considered to the blood flow through symmetric stenosis artery in steady flow simulations. The effect of blood flow variables and wall shear stress are related to viscoelasticity are more significant than the viscoelastic ones. The blood flow variables are predominant and increased with the flow rate decreased consequently at the throat of stenosis. The choice of the characteristic viscosity μ_n is main cause for the reference Newtonian and (non-generalized) Oldroyd-B solution. The apparent viscosity is close to μ_0 in the large part of vessel at low shear rates and the difference for the Newtonian solution at high flow rate. At present problem, the numerical method used to solve the governing equations seems to be sufficiently robust and efficient for the appropriate resolution. To derive and solve the governing equations, the finite element method and iteration method has been applied for velocity component, pressure, tensor component and wall shear stress by considering Weissenberg numbers of 0.0, 0.5 and 1.00 and Reynold numbers of 10^2 to 10^3. The following outcomes of the research may also be useful in bio-medical engineering.

(i) The effect of blood flow variables have more significant changed at the throat of stenosis for all four models.

(ii) In blood flow, the effect of dimensionless number Re and Wi are remarkable and flow variables are more affected at stenosis area. With increase of Wi the blood flow patterns and pressure distribution are almost alike for generalized Oldroyd-B model.

(iii) The wall shear stress effect on blood flow is an important factor in the onset of arterial diseases.

(iv) The maximum value of blood velocity and minimum value of blood pressure are found at second constriction region for all cases.

(v) The recirculation bubbles are originated at the throat of stenosis regions for all four models.

ACKNOWLEDGEMENTS

Authors would like to thank the Department of Information and Communication Technology (ICT), Bangladesh University of Professionals (BUP), for providing computer and other facilities during this work. We also express our gratitude to anonymous reviewers for their suggestions which improved the quality of the manuscript.

REFERENCES

1. Anand M and Rajagopal K R (2004), "A shear-thinning viscoelastic fluid model for describing the flow of blood", International Journal of Cardiovascular Medicine and Science, 4(2): 59–68.
2. COMSOL Multiphysics (2013), 4.3a users guide.
3. D' Elia M, Perego M and Veneziani A (2011), "A variational Data Assimilation procedure for the incompressible Navier-Stokes equations in hemodynamics*",* J. Sci. Comput, 52(2): 340-359.
4. Dechaumphai P (1995), "Adaptive finite element technique for heat transfer problems, Energy", Heat & Mass transfer, 17(2): 87-94.
5. Dechaumphai P (1999), Finite Element Method in Engineering, 2nd edition, Chulalongkorn University Press.
6. Keslerova R and Karel K (2015), "Numerical modelling of viscous and viscoelastic fluids flow through the branching channel", Programs and Algorithms of Numerical Mathematics, Institute of Mathematics AS CR, 100-105.
7. Kumar B R, Kumar G.A and Kumar S M (2010), MATLAB^{R} and its Application in Engineering, 2nd Edition, Panjab University.
8. Leuprect A and Perktold K (2001), "Computer simulation of non-Newtonian effects of blood flow in large arteries", Computer Methods in Biomechanics and Biomechanical Engineering, 4: 149–163.
9. Lowe D (1998), Clinical Blood Rheology, 1st Edition, CRC Press.

10. Mahfoud M and Benhadid S (2016), "Numerical study of the non-Newtonian blood flow in a stenosed artery using two rheological models", Thermal Science, 20(2): 449-460.
11. Marshall I, Zhao S, Sopoulou P P, Hoskins P and Xu X Y (2004), "MRI and CFD studies of pulsatile flow in healthy and stenosed carotid bifurcation models," Journal of Biomechanics, 37(5): 679–687.
12. Oka S (1973), "Pressure development in a non-Newtonian flow through a tapered tube," Biorheology, 10(2): 207–212.
13. Prokop V and Kozel K (2013), "Numerical simulation of Generalized Newtonian and Oldroyd-B Fluids", Numerical Mathematics and Advanced Application, 579-586, DOI 10.1007/978-3-642-33134-3 61.
14. Rajagopal K R and Srinivasa A R (2011), "A Gibbs-potential-based formulation for obtaining the response functions for a class of viscoelastic materials", Proc. R. Soc. A, 467: 39-58.
15. Robertson A M, Sequeira A and Owens R G (2009), "Rheological models for blood", in: Formaggia, L., Quarteroni, A., Veneziani, A. (Eds.), "Cardiovascular Mathematics, Modeling and simulation of the circulatory system" MS&A, Modeling, Simulations & Applications, 1: 211–241.
16. Taylor C and Hood P (1973), "A Numerical Solution of the Navier-Stokes Equations Using Finite Element technique", Computer and Fluids, 1(73). doi:10.1016/0045-7930(73)90027-3.
17. Telma G, Jorge T and Adelia, S. (2014), "Optimal control in blood flow simulations", Int. Journal of Non-Linear Mechanics, 64: 57-69.
18. Thurston G B (1973), "Frequency and shear rate dependence of viscoelasticity of blood", Biorheology, 10(3): 375-381.
19. Tu C and Deville M (1996), "Pulsatile flow of non-Newtonian fluids through arterial stenoses," Journal of Biomechanics, 29(7): 899–908.
20. Uddin N M and Alim M A (2017), "Numerical Study of Blood Flow through Symmetry and Non-Symmetric Stenosis Artery under Various Flow Rates", IOSR Journal of Dental and Medical Sciences, 16(6): 106-115.
21. Verdier C (2003), "Rheological properties of living materials. from cells to tissues", Journal of Theoretical Medicine, 5(2): 67–91.